International Journal of Control, Automation and Systems 15(2) (2017) 918-932
http://dx.doi.org/10.1007/s12555-015-0271-0
ISSN:1598-6446 eISSN:2005-4092
http://www.springer.com/12555

From Single to Many-objective PID Controller Design using Particle Swarm Optimization

Hélio Freire*, P. B. Moura Oliveira, and E. J. Solteiro Pires

Abstract: Proportional, integrative and derivative (PID) controllers are among the most used in industrial control applications. Classical PID controller design methodologies can be significantly improved by incorporating recent computational intelligence techniques. Two techniques based on particle swarm optimization (PSO) algorithms are proposed to design PI-PID controllers. Both control design methodologies are directed to optimize PI-PID controller gains using two degrees-of-freedom control configurations, subjected to frequency domain robustness constraints. The first technique proposes a single-objective PSO algorithm, to sequentially design a two degrees-of-freedom control structure, considering the optimization of load disturbance rejection followed by set-point tracking optimization. The second technique proposes a many-objective PSO algorithm, to design a two degrees-of-freedom control structure, considering simultaneously, the optimization of four different design criteria. In the many-objective case, the control engineer may select the most adequate solution among the resulting optimal Pareto set. Simulation results are presented showing the effectiveness of the proposed PI-PID design techniques, in comparison with both classic and optimization based methods.

Keywords: Evolutionary algorithms, many-objective optimization, particle swarm optimization, PID control.

1. INTRODUCTION

The relevance of PID control within industrial feedback loops has been a major motivational aspect to the development of a wide range of appropriate design techniques. A well established technique of classical design methodologies, once the controller type is selected (P, PI, PD or PID), rely on the use of tuning rules to evaluate the respective controller gains. Many of these tuning methods were developed considering a specific control design objective and control configuration [1]. Two of the most significant classical control objectives are set-point tracking (SPT) and disturbance rejection (DR). Thus, many tuning rules were developed by optimizing time domain transient response criteria regarding these two design objectives. However, tuning rules for SPT can result in poor DR, and vice-versa. Moreover, many design techniques were developed for specific process dynamics [1–6]. Besides SPT and DR criteria, PID controller should be designed considering other criteria such as robustness, controller effort, noise rejection, etc. Some of the former design criteria are difficult to be adequately accommodated by classical design techniques such as to achieve a good compromise between robustness and performance. To circumvent this limitation, optimization techniques can be integrated in the controller design methodology, such as the convex-concave formulation proposed in [7].

Nature and biologically inspired techniques have been successfully applied to design PID controllers. Examples of some established techniques which have been applied to this purpose considering single and multiple objectives are: genetic algorithm [8–11], particle swarm optimization [12–15], differential evolution [16], gravitational search algorithm [17], etc.

In this work, the problem of designing PID controllers with minimum robustness characteristics is addressed by proposing two different techniques based on particle swarm optimization:

1) A single-objective technique, in which the controller design is accomplished by minimizing a time-domain cost function subjected to robustness constraints. The design procedure is based on two sequential steps: i) optimization for minimum integral of time square error (ITAE) for load disturbance rejection; ii) improvement of SPT with a two degrees-of-freedom configuration. This part is an extension of the authors work previously reported in [18].
2) A many-objective technique, considering, simultaneously, the optimization of four design objectives. The

Manuscript received July 9, 2015; revised November 27, 2015 and March 1, 2016; accepted March 22, 2016. Recommended by Associate Editor Yangmin Li under the direction of Editor Euntai Kim. This work was supported by the *Fundação para a Ciência e a Tecnologia* (FCT) under PhD studentship No. SFRH/BD/79463/2011.
Hélio Freire, Paulo Oliveira and E.J. Solteiro Pires are with the School of Sciences and Technology, INESC-TEC - UTAD pole, UTAD University, 5000-801 Vila Real, Portugal (e-mails: freireh@gmail.com, {oliveira, epires}@utad.pt).
* Corresponding author.

aim is to obtain a set of non-dominated solutions that represents different optima from which the decision maker can choose the solution that better suits to its problem. The objectives considered in this study are: i) minimization of ITAE for SPT, ii) minimization of ITAE for load DR, iii) minimization of the control effort (CE) and iv) maximization of the Vector Margin (VM). The technique originally proposed by the authors in [19] is extended and adapted here to the robust PID controller design problem. Single and multi-objective PSO algorithms have been widely applied to PID controllers design [10, 20, 21], however when the number of objectives is higher than three (many-objective) the problem complexity increases significantly and so far the number of related publications is scarce.

Indeed, concerning many-objective design problems, there is the urge to develop new effective design techniques with practical application. So, the motivation of this work is to propose: a single objective PSO based optimization technique to design robust PID controllers, as an alternative to concave-convex optimization. A Many-Objective Particle Swarm Optimization technique to PID controller design problems. As reported in the authors previous work [22], Corner Based many-objective optimization technique performs better than three well established reference techniques: NSGAII (Non-dominated Sorting Algorithm II) [23], SMPSO (Speed constrained Multi-objective PSO) [24] and GDE3 (third Evolution Step of Generalized Differential Evolution) [25]. The reported results in [22] consider 4 to 10 different objectives for 5 benchmark many-objective functions.

The remainder of the paper is structured as follows: Section 2 presents some key issues to design PI-PID controllers. Section 3 presents a single objective PSO based technique to design PID controllers. Section 4, presents the many-objective algorithm to design PID controllers. In Section 5 simulation results are presented and analysed. Finally, Section 7 presents some concluding remarks.

2. PI-PID CONTROLLERS: OVERVIEW OF FUNDAMENTAL ASPECTS

This section presents key aspects to design PI-PID controllers using an optimization approach. Some of the main control design objectives can be easily perceived by considering a generic single-input single-output system block diagram represented in Fig. 1 where r represents the reference input (set-point), y the controlled output, d_1 the load disturbance, d_2 the output disturbance, n the noise signal, u the controller output, G_c the controller transfer function, and G_p the system or process to control. The global problem consists in designing the controller, such as the output signal y tracks as close as possible the reference input

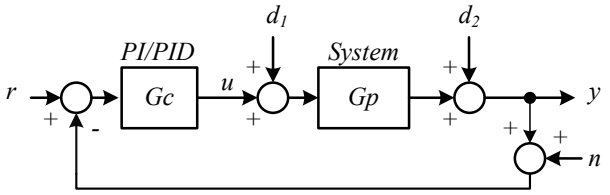

Fig. 1. General feedback loop.

(set-point tracking), while rejecting as much as possible any signal disturbance and noise. The controller design should also consider robustness issues, to be further detailed in this paper. PID controllers can be represented by different equations depending on the implementation approach used. In this study, the parallel form represented respectively by (1) and (2), for the PI and PID controller will be deployed.

$$G_{cPI}(s) = K_p\left[1+\frac{1}{sT_i}\right] = K_p + \frac{K_i}{s}, \quad (1)$$

$$G_{cPID}(s) = K_p\left[1+\frac{1}{sT_i}+sT_d\right] = K_p + \frac{K_i}{s} + sK_d, \quad (2)$$

where $K_p, T_i, T_d, K_i = K_p/T_i$ and $K_d = K_pT_d$, represent respectively, the proportional gain, integrative time constant, derivative time constant, integrative and derivative gains. In practice, since equation (2) is a non-proper transfer function, it cannot be physically implemented, requiring alternative formats [1] such as using a derivative action filter. It is also common to use a first order (or second order) filter in series with the PID controller resulting in the following expression:

$$G_c(s) = G_{cPID}(s)G_{ft}(s) = K_p\left[1+\frac{1}{sT_i}+sT_d\right]\left[\frac{1}{1+sT_f}\right] \quad (3)$$

with G_{ft} representing the filter transfer function and T_f the respective time constant. Recently, significant research efforts have been devoted to reject the noise in the designing of PID controllers [26, 27]. It is a common approach to obtain the optimum (or near-optimum) controller settings by applying a step signal either to the reference input or load DR and measure the performance in the time-domain using the well-known integral of absolute error (IAE):

$$IAE = \int_0^\infty |e(t)|dt, \quad (4)$$

or the integral of time weighted absolute error (ITAE):

$$ITAE = \int_0^\infty t|e(t)|dt. \quad (5)$$

The control effort (CE) should be as minimum as possible. One way to evaluate the control effort is using:

$$CE = \int_0^\infty |u(t)|dt \quad (6)$$

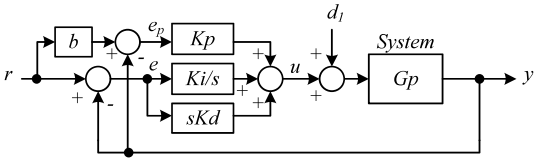

Fig. 2. PID control with set-point weighting.

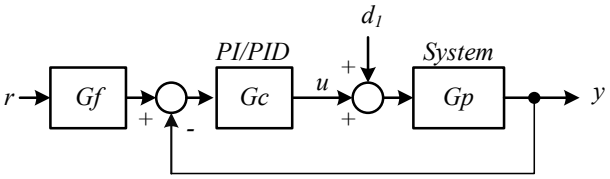

Fig. 3. PI/PID control with a feedforward pre-filter.

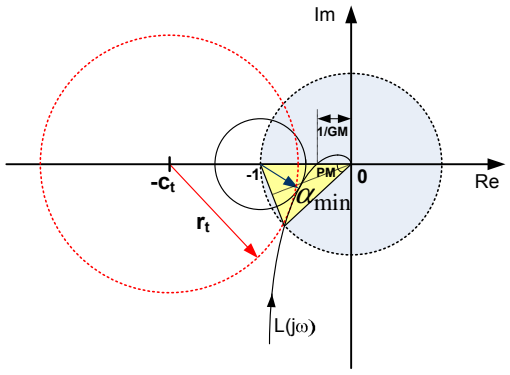

Fig. 4. Loop Nyquist plots with circles constraints.

while another common way to evaluate the control signal smoothness is with the total variation (TV) defined using a discretization of the respective continuous signal as [4]:

$$TV = \sum_{i=0}^{\infty} |u_{i+1} - u_i| \tag{7}$$

with u representing the controller output discrete vector. As stated previously, when the PID controller is designed to achieve the optimum load disturbance rejection, these gains often results in poor SPT performance, namely in terms of first overshoot. To improve the set-point tracking response while maintaining the feedback loop disturbance properties, two degrees-of-freedom configurations can be used [28]. The general idea is to use a second controller which usually is of a feedforward type. A very successful and established technique is known as set-point weighting [29], consisting in assigning a weight b, to the set-point value in the error input to the proportional part (see Fig. 2 for the PID controller). In this case, the error term for the proportional component, e_p, is different from the standard error applied to the integral and derivative components, e:

$$e_p(t) = br(t) - y(t), \tag{8}$$
$$e(t) = r(t) - y(t). \tag{9}$$

It can be shown that the configuration presented in Fig. 2 is equivalent to a classical two degrees-of-freedom configuration with a feedforward prefilter, G_f, applied to a referenced input outside the feedback loop as shown in Fig. 3, represented for the PI and PID controller, respectively by:

$$G_{fPI}(s) = \frac{bK_p s + K_i}{K_p s + K_i}, \tag{10}$$
$$G_{fPID}(s) = \frac{bK_p s + K_i + K_d s^2}{K_p s + K_i + K_d s^2}. \tag{11}$$

In the former feedforward PI equation, G_{fPI}, can be represented in a format of a classic lead-lag compensator:

$$G_{fPI}(s) = \frac{bT_i s + 1}{sT_i + 1} = \frac{sT_{lead} + 1}{sT_{lag} + 1} \tag{12}$$

with $T_{lead} = bT_i$ and $T_{lag} = T_i$.

Concerning the robustness issues, the design follows the use of frequency-domain Nyquist plots circle constraints as proposed in [7], which will be described based on the illustrative example presented in Fig. 4. In this figure: $L(\mathrm{j}\omega) = G_c(\mathrm{j}\omega)G_p(\mathrm{j}\omega)$ represents the loop frequency response, $\alpha_{\min}$ represents the vector margin [30,31] whose magnitude corresponds to the minimum distance between the point $-1 + j0$ and the loop polar plot, GM and PM the gain and phase margin, respectively, c_t and r_t, represent the complementary sensitivity circle center and radius, respectively. Two very convenient relations between the vector margin and the gain and phase margins are represented by:

$$GM \geq \frac{1}{1 - \alpha_{\min}}, \tag{13}$$
$$PM \geq 2\arcsin\left(\frac{\alpha_{\min}}{2}\right). \tag{14}$$

Considering that the sensitivity function is defined by:

$$S(\mathrm{j}\omega) = \frac{1}{1 + L(\mathrm{j}\omega)} \tag{15}$$

the relation between the maximum sensitivity value, Ms, and the vector margin can be established by:

$$M_s = \max|S(\mathrm{j}\omega)| = \frac{1}{\min|1 + L(\mathrm{j}\omega)|} = \frac{1}{\alpha_{\min}} \Rightarrow$$
$$\Rightarrow \alpha_{\min} = \frac{1}{M_s} = VM. \tag{16}$$

Determining the vector margin from (16) enables to obtain two estimates for both gain and phase margins (13, 14). Another classic robustness measure is the maximum

Table 1. Relation among M_s, vector margin, gain and phase margins. Relation among M_t and circle center (c_t) and radius (r_t).

Example	M_s	VM	GM	PM	M_t	c_t	r_t
1	1.20	0.83	6.00	49.25°	1.20	−3.27	2.73
2	1.40	0.71	3.50	41.85°	1.40	−2.04	1.46
3	1.60	0.63	2.67	36.42°	1.60	−1.64	1.03
4	1.80	0.56	2.25	32.26°	1.80	−1.45	0.80
5	2.00	0.50	2.00	28.96°	2.00	−1.33	0.67

complementary sensitivity value, M_t, represented in the following expression:

$$T(\mathrm{j}\omega) = \frac{L(\mathrm{j}\omega)}{1+L(\mathrm{j}\omega)}, \quad M_t = \max|T(\mathrm{j}\omega)| \tag{17}$$

The maximum complementary sensitivity value is related with another circle in the Nyquist plot defined by, center, c_t, and radius, r_t, evaluated with [7]:

$$c_t = -\frac{M_t^2}{M_t^2-1}, \tag{18}$$

$$r_t = -\frac{M_t}{M_t^2-1}. \tag{19}$$

In order to illustrate the relation among maximum sensitivity values, vector margin, gain and phase margins as well as among maximum sensitivity values and the respective circle center and radius, some examples are presented in Table 1. The overall objective is to design a PI/PID controller for which the corresponding loop Nyquist plot is outside both circles, which is formulated using these circles constraints within the optimization problem [7]. As it can be seen from Fig. 4, while the vector margin constraint is very useful to ensure minimum values for gain and phase margins, the M_t circle may complement the loop shaping procedure in lower frequency ranges. As shown in Table 1, lower values of M_t correspond to larger circle radius.

3. SINGLE-OBJECTIVE PI-PID CONTROLLER DESIGN USING PSO ALGORITHM

A classical particle swarm optimization algorithm [32] is deployed here as a simple tool to design PID controllers subjected to robustness circle constraints. This selection is based in the standard PSO algorithm implementation simplicity. However, refined PSO versions can be deployed as well (*e.g.* [33] and [34]). Two fundamental PSO equations governing the swarm particles dynamics are:

$$\begin{aligned} v_i(t+1) = {} & \omega v_i(t) + c_1\varphi_1[p_{best_i}(t) - x_i(t)] \\ & + c_2\varphi_2[g_{best}(t) - x_i(t)], \end{aligned} \tag{20}$$

$$x_i(t+1) = x_i(t) + v_i(t+1) \tag{21}$$

with: i representing the swarm element, t representing the iteration number, ω the inertia weighting factor, c_1 and c_2 the cognitive and social constants, respectively, φ_1 and φ_2 represent two randomly generated numbers with uniform distribution in the range [0,1]. In this case $c_1 = c_2 = 2$ is considered. In equation (20) p_{best_i} represents the best individual value, found so far, for each particle and g_{best} the global best particle of the entire swarm or specified neighbourhood. Position and velocity vectors are d-dimensional. The inertia weight is usually decreased linearly (or otherwise as reported in [35]) between a maximum starting value and a minimum ending value. The velocity values evaluated with (20) are used to update the particle positions (21). The PSO stopping criterion adopted here is a pre-established number of iterations. The proposed approach consists in a single objective optimization using as criterion the ITAE (5) index minimization subjected to vector margin and complementary sensitivity robustness constraints. Each swarm member encodes the controller parameters: $\{K_p, K_i\}$ or $\{K_p, K_i, K_d\}$ for the PI or PID case, respectively. The design methodology proposed can be described by the following sequential steps:

1) Design the PI-PID controller to obtain good controller gain settings for the objective of load disturbance rejection. Vector margin (16) and complementary sensitivity value (17) are used as constraints.
2) Using the controller gains obtained in step 1, design the feedforward controller to improve the SPT response, by either using a set-point weighting approach or a more flexible lead-lag feedforward pre-filter.

Three relevant remarks regarding specific PSO implementation issues are:

- The swarm population is initialized using an interview method that consists in generating elements randomly until stable controllers are found, *i.e.*, unstable controllers are not allowed to incorporate the initial swarm. This procedure is relevant to guarantee that all particles of the initial swarm result in stable control systems. This procedure is adopted as prior experimentation indicated that for some systems most (if not all) randomly generated elements represent unstable controllers.
- During the PSO execution, particles representing controller setting violating the robustness constraints are penalized as described by the cost functions represented by (22 - 23), where $VM_{\min}$ represents the minimum value for the vector margin, $M_{t_{\max}}$ the maximum value for M_t, γ_1 and γ_2 representing penalizing weighting factors. The higher the values assigned

to the penalizing factors the less influence the corresponding particles will be in the PSO search.

$$if \quad VM < VM_{\min} \Rightarrow cost_{VM} = \gamma_1 |VM - VM_{\min}|, \tag{22}$$

$$if \quad M_t \geq M_{t_{\max}} \Rightarrow cost_{M_t} = \gamma_2 |M_t - M_{t_{\max}}|. \tag{23}$$

- The controller design for load DR attaining certain robustness margins may enable the SPT improvement with the set-point weighting approach. However, minimizing the ITAE for SPT with the fixed feedback loop while improving ITAE may result in high values of overshoot. Thus, the following constraint is used to promote smaller overshoot values.

$$if \quad M_p \geq M_{p_{\max}} \Rightarrow cost_{M_p} = \gamma_3 |M_p - M_{p_{\max}}|. \tag{24}$$

  M_p represents the first overshoot. $M_{p_{\max}}$ the maximum overshoot and γ_3 a penalizing constant.
- The overall cost is given by ITAE and the penality function:

$$cost = ITAE + cost_{VM} + cost_{M_t} + cost_{M_p}. \tag{25}$$

4. FROM SINGLE-OBJECTIVE TO MANY-OBJECTIVE PSO (MaPSO)

4.1. Concepts of evolutionary many-objective optimization

A minimization problem can be formulated as (26) [36]:

$$\begin{aligned} &\min f(\mathbf{x}) = (f_1(\mathbf{x}), f_2(\mathbf{x}), ..., f_m(\mathbf{x})) \\ &\quad s.t. \quad g_l(\mathbf{x}) \leq 0, \quad l = 1, 2, ..., k \\ &\quad \mathbf{x} \in \mathbf{S} \subset \Re^n, \end{aligned} \tag{26}$$

where $\mathbf{x} = (x_1, x_2, ..., x_n)$ is a n-dimensional decision variable, $g_l(\mathbf{x})$, $l = 1, 2, ..., k$ represents the lth constraint, and $f_j(\mathbf{x}), j = 1, 2, ..., m$, is the jth objective function where m represent sthe number of objectives to be optimized. When the value of m in (26) is greater than three, is considered a Many-Objective Optimization Problem (MaOP).

Definition 1 (Pareto Dominance)**:** Given two solutions, $\mathbf{x}, \mathbf{y}$, it said that $\mathbf{x}$ dominates $\mathbf{y}$ (denoted by $\mathbf{x} \prec \mathbf{y}$) if solution $\mathbf{x}$ is not worse than $\mathbf{y}$ in all objectives, $f_i(\mathbf{x}) \leq f_i(\mathbf{y})$ and if at least one objective $f_i(\mathbf{x}) < f_i(\mathbf{y})$ for $i = 1, \ldots, M$.

Definition 2 (Maximin)**:** Maximin [37] is an algorithm used when the solutions in the front are more than the available slots in the archive. The objective is to select the solutions for a better distribution in the Pareto front. Initially, the extreme solutions are selected and inserted in the archive and removed from the front. Then, in a recursive way, the minimum distance between each solution is calculated in the front and the solutions which are already in the archive and, in every iteration, the solution with the higher distance value is chosen. This solution is removed from the front and inserted in the archive. This process is repeated until the archive is full.

Definition 3 (Corner Solutions)**:** Corner Solutions are solutions in the Pareto front where the boundaries intersect. These solutions represent the maximum value for an objective when the others have minimum values.

One of the main streams used to adapt single objective optimization algorithms to multi-objective optimization algorithms, is directed to achieve a set of solutions that respect the concepts of the Pareto dominance. More concepts of Pareto optimal set and Pareto front, well known by now, can be found in [38]. The multi-objective PSO algorithms addressed in this work are also based on non-dominated Pareto optimality concepts. The Multi-objective PSO formulation use the same equations, (20) and (21), of the single-objective PSO. However, while for a standard single-objective non-multimodal search space the aim is to find the single optimum, in this multi-objective approach the aim is to obtain a set of non-dominated solutions. Thus, when PSO is extended to Multi-Objective Problems (MOPs) some crucial aspects must be addressed such as: the process of selecting non-dominated particles; How to update the global and the local best particles? How to maintain the diversity of an archive swarm? After each particle evaluation, based on Pareto dominance principles, the swarm particles are candidates to belong to the archive. As the archive is limited in its capacity, it's necessary to have methods to select the best ones. Normally at this stage, the promotion of the population diversity is privileged. The main multi-objective optimization concerns can be stated as to [39]:

- Preserve non-dominated points in the objective space.
- Continue to make algorithmic progress towards the Pareto Front in objective function space.
- Maintain diversity of non-dominated points.
- Provide the decision maker 'enough' but limited number of Pareto solutions for corresponding decision variable values for a given problem.

The key aspects which justify the significant complexity increase, in many-objective optimization, due to the increase of the number of the criteria considered, are related with the following:

- A high percentage of non-dominated solutions at early stages. This aspect affects the ability of algorithms to converge for the global Pareto front.
- As the number of objectives grow, more solutions are necessary to cover the global Pareto optimal front.
- The visualization of non-dominated solutions is more difficult with the increase of objective number because the required projections in a two or three dimensional graph.

$t \leftarrow 1$;
Randomly generate the swarm $pop(t)$ of $npop$ particles;
repeat
  Validate $pop(t)$;
  Fill archive;
until *stopping condition is reached*;
Initialize the corner archive;
STEP 1
repeat
  Update swarm;
  Evolve swarm;
  Update archive;
  Update corner archive;
  $t \leftarrow t+1$;
until *stopping condition is reached*;
STEP 2
repeat
  Update swarm;
  Evolve swarm;
  Update archive;
  $t \leftarrow t+1$;
until *stopping condition is reached*;

Algorithm 1: MaPSO algorithm for PID design

4.2. The proposed MaPSO algorithm

The many-objective algorithm proposed to solve the PID robust design problem is presented in Algorithm 1.

Many-objective optimization problem solving can be a difficult task. Algorithm 1 is based in the algorithm proposed in [22]. In this work the swarm particles are initially generated randomly. Therefore, a significant number of the randomly initialized particles can represent unstable controller solutions. In this case, if at least 5% of particles in the swarm do not represent stable controllers it is necessary to repeat the process with unstable particles set until 5% of stable controllers are met. These stable particles are kept in the archive. Then, based in the particles kept in the archive, a corner archive is built, in which one solution for each corner (also known as extreme solutions) are stored. In Step 1, of Algorithm 1, the main goal is to find the corner particles. These corner particles are the candidates to g_{best} particles. Step 2, of Algorithm 1, privileges the solutions diversity. Then, based in the Pareto principles of non-dominance the particles are kept in the archive. These particles will be the final solutions presented in the next section. The general archive has limited space. As in this work an archive with 20 solutions of capacity is deployed, when candidates to integrate the archive are larger than 20, the maximin [37] selection procedure is used.

Another very relevant issue is how the swarm particles select their g_{best} particle. All the solutions in the archive can be a potential g_{best} particle. For each particle in the swarm two particles of the archive are selected randomly, and from these two particles the nearest particle to the swarm particle is selected as the respective g_{best}. The distances are evaluated in the objective space. The p_{best} leaders are replaced if the new particle dominated the existing ones.

Other parameters of the tests are: i) Number of particles in swarm: 100; ii) Max number of iterations: 50.

The archive solutions have to keep the control design robustness constrains: VM be equal or greater than 0.5 and M_t be equal or smaller than 1.76.

The technique deployed here to design PID controllers, considers the following design criteria:

1) SPT by minimizing the ITAE (5): a unit step is applied solely to reference input signal: $(r(t) = 1, d(t) = 0)$.
2) Load DR by minimizing the ITAE (5): a unitary step is applied solely to the load disturbance input signal: $(r(t) = 0, d(t) = 1)$.
3) Minimization of Control effort, by minimizing (6) when $(r(t) = 1$ at $t = 0s$, $d(t) = 1$ at $t =$ half the simulation time).
4) Maximization of Vector Margin, by maximizing VM, (16). The Vector Margin restriction was set to a lower minimum value of 0.5.

5. SIMULATION RESULTS AND DISCUSSION

5.1. Single-objective PI-PID design

Two models used in [7] are considered in this study representing an open-loop unstable system, G_{p1} (27), and a triple pole system, G_{p2} (28):

$$G_{p1}(s) = \frac{1}{(s-1)(0.1s+1)}, \tag{27}$$

$$G_{p2}(s) = \frac{1}{(s+1)^3}. \tag{28}$$

The control objective considered consists in optimizing the system load rejection response when a unit step input disturbance and the reference input with no signal applied. The PSO conditions used are: swarm size $m = 30$, 60 iterations, and ω was linearly decreased between 0.9 and 0.4. The penalizing weights were set to $\gamma_1 = \gamma_2 = \gamma_3 = 20$ in (22), (23), and (24). These values were selected by prior experimentation. However, other higher values penalizing solutions which violate the defined constraints will work as well. PI controller parameter range used was [0.1, 20] for K_p and K_i. In the case of the PID controller the range for the proportional and integrative gains are the same as for the PI case and the range for K_d is [0.1, 20]. All simulations were carried out in Matlab/Simulink environment assuming the simulation time to be shown in the time-response plots, with a fixed solver step interval of 0.01s. PI control was applied to G_{p1} system and PID control to G_{p2} system.

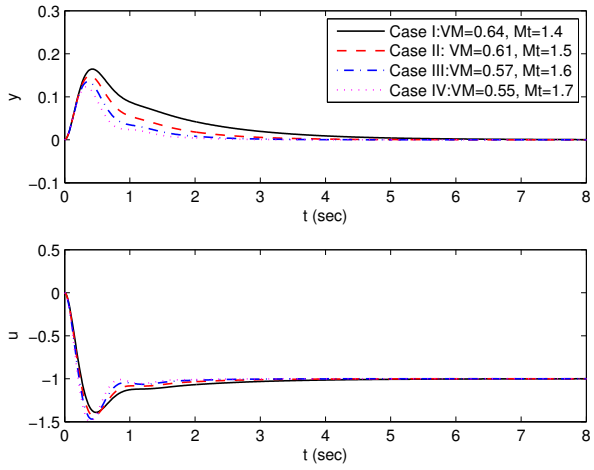

Fig. 5. PI control results for system G_{p1}. Load disturbance step responses.

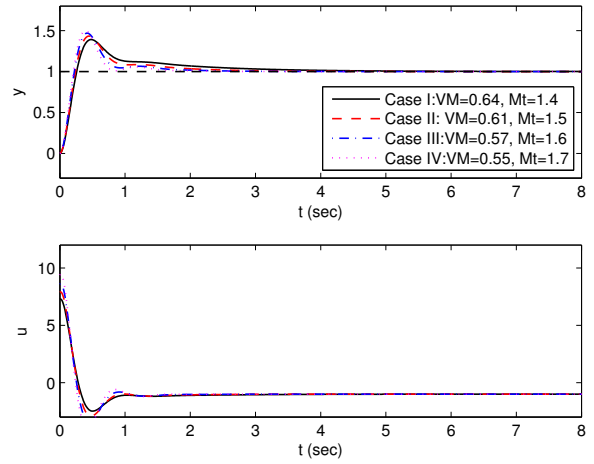

Fig. 6. PI control results for system G_{p1}. Set-point tracking responses.

Table 2. PI gains obtained using the PSO for system G_{p1}.

Case	K_p	K_i	ITAE	TV	VM	M_s	M_t
I	7.28	4.35	0.33	1.78	0.64	1.56	1.4
II	7.87	7.03	0.14	1.87	0.61	1.64	1.5
III	8.58	9.94	0.08	1.98	0.57	1.75	1.6
IV	9.34	13.06	0.05	2.10	0.55	1.82	1.7

Table 3. PID gains obtained using the PSO for system G_{p2}.

Case	K_p	K_i	K_d	ITAE	TV	VM	M_s	M_t
I	3.89	2.59	3.85	1.76	1.33	0.71	1.41	1.15
II	5.86	4.38	5.32	0.89	1.60	0.63	1.59	1.27
III	8.24	7.25	7.11	0.50	1.92	0.56	1.79	1.51
IV	10.96	11.44	9.02	0.30	2.26	0.50	2.00	1.76

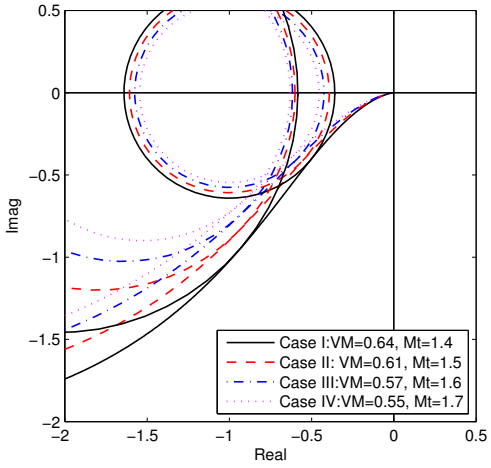

Fig. 7. PI control results for system G_{p1}. Nyquist plots with circles constraints.

The results obtained are presented in Figs. 5, 6, and 7 and in Tables 2 and 3, for 4 different cases represented by (I to IV). As for system G_{p1}, the most influential constraint in the response is M_t constraint, a fixed $VM = 0.5$ was used for all the 4 cases. The M_t values considered were $\{1.4, 1.5, 1.6, 1.7\}$ corresponding respectively to cases I to IV. Fig. 5 presents the load unit step response, with the top plot representing the system output signal (y) and the lower part the controller output signal (u) for the depicted cases. Fig. 6 presents the SPT response for the same cases presented in Fig. 5. Fig. 7 presents the Nyquist plots with the corresponding vector margin (VM) and M_t circles. As it can be observed the VM value obtained is always superior to the defined minimum, of $VM = 0.5$ and as the M_t is increased the load DR improves and the control effort increases. The improvement in terms of the ITAE criterion with the M_t increase can be observed by the corresponding decreased values presented in Table 3. The values obtained for TV indicates that the control effort increase corresponds to a TV increase, but not significant as the control signal smoothness is maintained.

Fig. 8 shows a comparison of the results obtained with the PSO with the results reported in [7] for G_{p1}, considering a vector margin $VM = 0.714$ (equivalent to $Ms = 1.4$) and $Mt = 1.4$. This is denoted as case V in Fig. 8, and the gains obtained with the PSO algorithm were $Kp = 4.84$ and $Ki = 2.00$ while the gains obtained in [7] are $Kp = 4.67$ and $Ki = 1.76$. As it can be observed the results are very similar, slightly better for the PSO case, showing that this simple algorithm can be used to design PI controller as an alternative to concave-convex optimization. The SPT tracking performance can be improved by using a set-point weighting pre-filter represented by (10).

The results of optimizing the pre-filter using the PI gains obtained for case II are presented in Fig. 9 for two

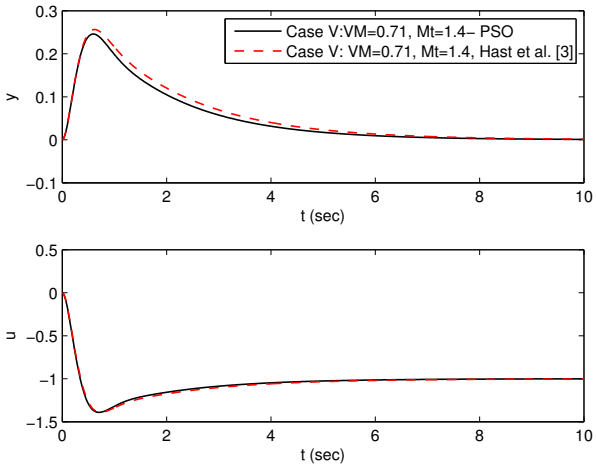

Fig. 8. PI control results for system G_{p1}. Comparison with the results obtained in [7]

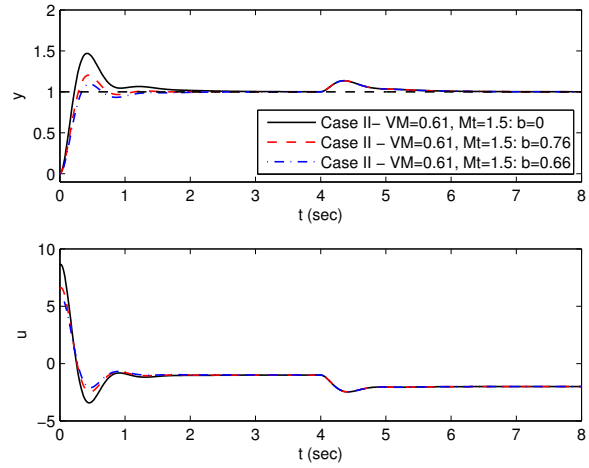

Fig. 9. PI control results for system G_{p1} with set-point weighting. Set-point tracking responses.

cases. In the case of $b = 0.76$ the optimization was performed without any constraint (23) penalizing the overshoot. In the case of $b = 0.66$, the ITAE is worse than for the case of $b = 0.76$, as a constraint was used penalizing overshoots higher than 5%. Fig. 9 also shows that the improvements of the SPT tracking response are independent of the DR, as expected. In the case of $b = 0.66$ the same results can be obtained by using a two degrees-of-freedom configuration with $T_{lead} = bT_i = 0.66 \times 1.76 = 1.16s$ and $T_{lag} = T_i = 1.76s$.

The results achieved for PID control are presented in Figs. 10-13 and Table 3, in the same format used for PI control. For system, G_{p2}, the most influential constraint is the vector margin. Thus M_t was made constant with a minimum value of 1.1 for all cases. The VM values considered were $\{0.71, 0.63, 0.56, 0.5\}$ corresponding respectively to cases I to IV. The correspondences between these VM values and the M_s values are presented in Table 1. The results presented for this plant, show that the PSO can exactly match the specified constraint for all cases. In Fig. 13 the results of enhancing the SPT response with a set-point weighting using the pre-filter depicted in (11) for the PID. As it can observed the degree of improvement for the fixed DR PID gains are limited in this case. In Fig. 13, the response obtained with a lead-lag pre-filter governed by (12) is presented. As it can be observed the response is significantly improved. As in this case the load disturbance response is not independent for SPT, the load DR also improved by the use a lead-lag pre-filter and the achieved overshoot is ideal. The results of both examples indicates that PSO can easily accommodate robustness constraints to design robust PI-PID controllers, and constitute a simple and powerful alternative to other more complex optimization techniques, such the one presented in [7].

5.2. Many-objective PI-PID design

The same two models used in the single-objective case, (27) and (28), are considered in the many objective design. To maintain the coherence with the single objective optimization the results presented in this section concern:

- The PI controller is applied to control plant G_{p1}, using the two-degrees of freedom control configuration represented in Fig. 3, with the lead-lag feedforward pre-filter represented by (10). The optimization considers the four objectives formulated in section 4.2. Thus the controller parameters are $\{K_p, K_i, T_{lead}, T_{lag}\}$.
- The PID controller is applied to control plant G_{p2}, using the two degrees-of-freedom control configuration represented in Fig. 3, with the lead-lag feedforward pre-filter represented by (11). The optimization criteria considers the four objectives formulated in section 4.2. Thus, the controller parameters are $\{K_p, K_i, K_d, T_{lead}, T_{lag}\}$.

The results presented in this section were achieved running the proposed MaPSO algorithm with the following conditions: i) Swarm size: 100; ii) Archive size: 20; iii) Number of iterations per run: 50; iv) $\omega = 0.728$; v) $c_1 = c_2 = 2$.

All simulations were carried out in Matlab/Simulink environment assuming the simulation time to be shown in the time-response plots, with a fixed solver step interval of $0.01s$. The MaPSO was run ten times per system. The results presented represent the 20 non-dominated solutions obtained from merging the final archives using the maximin method [37]. However, the proposed MaPSO design method requires just one run.

The overall design for both cases is to achieve a Pareto front with optimum solutions regarding all four design objectives allowing the control engineer to select the most

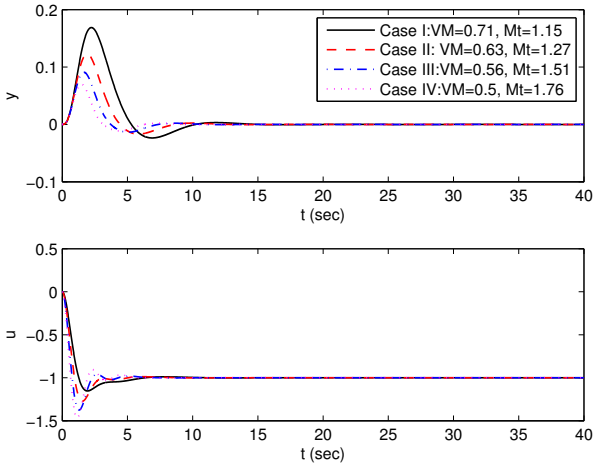

Fig. 10. PID control results for system G_{p2}. Load-step responses.

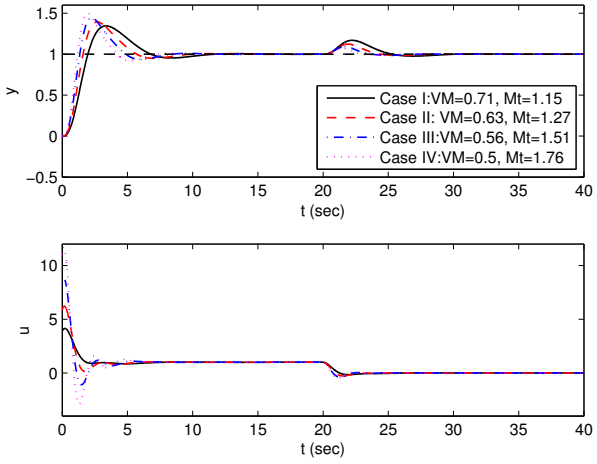

Fig. 11. PID control results for system G_{p2}. Set-point tracking responses.

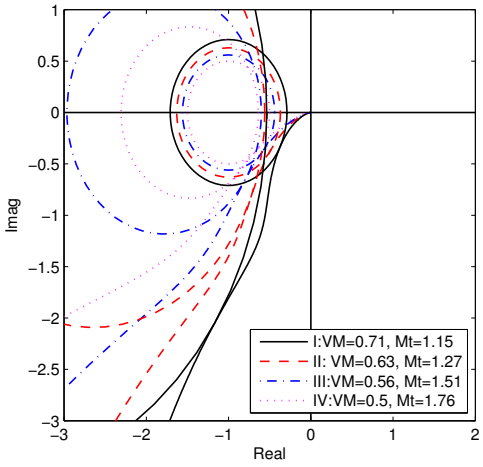

Fig. 12. PID control results for system G_{p2}. Nyquist plots with circles constraints.

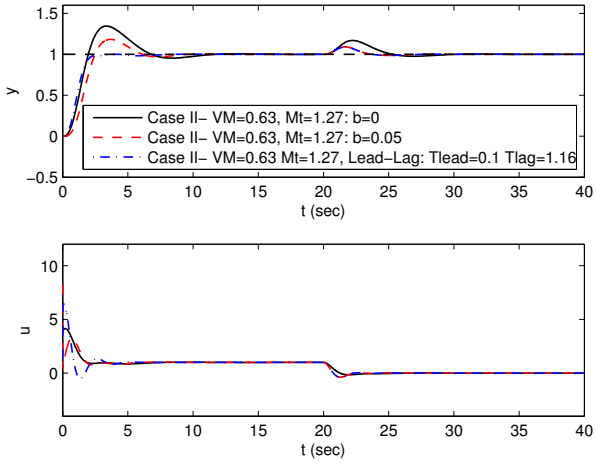

Fig. 13. PID control results for system G_{p2} with set-point filtering and lead-lag pre-filtering.

appropriate parameter set. The results obtained for plant G_{p1} are presented in Figs. 14 and 15 concerning a final non-dominated set with 20 solutions. Figs. 14 presents system output signals (y) to the SPT responses when a unit step is applied at $t = 0s$ and the load DR when a step is applied at $t = 10s$ and the corresponding PI controller output signal (u). Fig. 15 shows the Nyquist plots for all the final 20 controller solutions. In Fig. 15 besides the Nyquist polar plot for the 20 final solutions the VM and maximum complementary sensitivity circle constrains are presented. For the case of $VM = 0.71$ the M_t constrain is not indicated in the figure legend as it is the same as $M_t = 1.4$.

Table 4 presents the results achieved for the 20 non-dominated solutions, both in the parameter space and in the objective space, which represent a wide variation in terms of performance regarding the design criteria considered. Acting as the decision maker in this case, from the 20 PI controller solutions presented in Table 4, four solutions (shown in bold) were selected and the corresponding SPT response and load DR responses are presented in Figs. 16. The criteria used to select these four cases were: small values for the first overshoot, good performance rejecting the load disturbance and good robustness properties in terms of M_t and VM values. As it can be observed from Fig. 16, these four PI controller solutions present different trade-off between SPT, DR, and the CE. For instance, solution 1 has fast set-point tracking, small first overshoot and good DR, with the cost of demanding a higher control effort. On the other hand, solutions #4, #9 and #11, present slower SPT, no first overshoot, and worth DR, but better control effort value. Fig. 17 presents Nyquist plots for the selected 4 solutions. Concerning the robustness values, the better ones are solutions #9 and #11, and the worth ones are solutions #1 and #4. Table 4 shows that the 4 selected solutions presents quite low values for

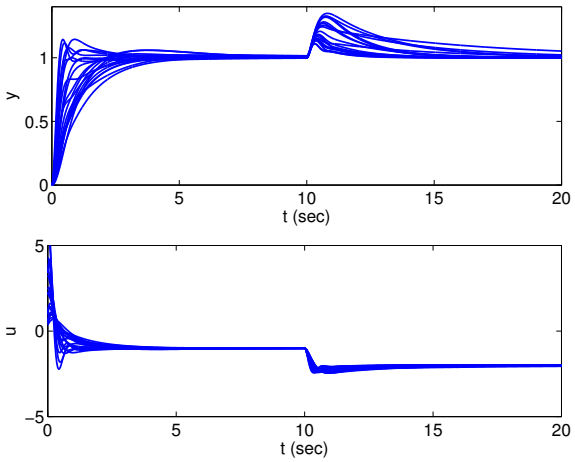

Fig. 14. G_{p1} results. SPT and DR response and Controller output signals for the 20 solutions.

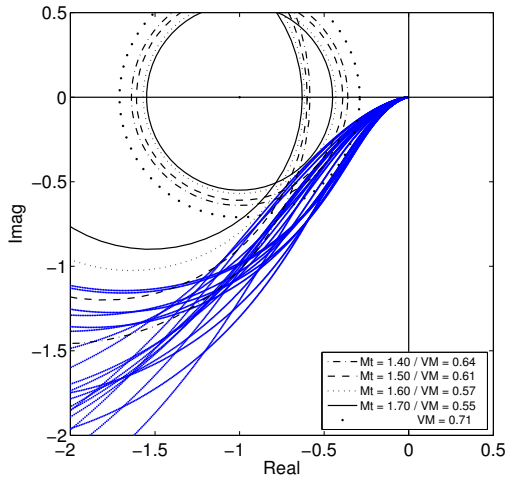

Fig. 15. G_{p1} results. Nyquist plots for the 20 final solutions.

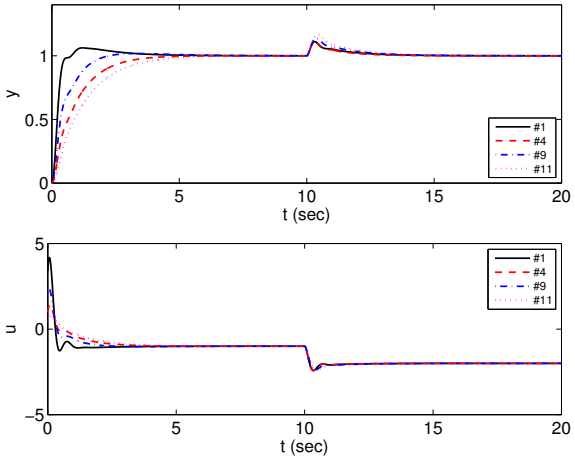

Fig. 16. G_{p1} results. SPT and Dr response and Controller output signal for the 4 selected solutions.

T_{lead} with a minimum variation for all four cases.

Table 4. Non-dominated front obtained by G_{p1}.

#	variables				objectives				M_s	M_t
	K_p	K_i	T_{lead}	T_{lag}	ITAE SPT	ITAE LDR	CE	VM		
1	**11.38**	**7.51**	**0.10**	**0.34**	**0.32**	**0.18**	**30.78**	**0.57**	**1.75**	**1.54**
2	8.61	5.59	0.10	1.23	0.87	0.24	29.02	0.61	1.63	1.44
3	6.55	3.52	0.10	1.12	0.86	0.45	29.43	0.66	1.52	1.38
4	**11.43**	**9.02**	**0.10**	**1.15**	**0.87**	**0.13**	**28.90**	**0.56**	**1.78**	**1.58**
5	3.94	1.01	0.99	2.81	2.41	2.88	30.03	0.74	1.35	1.43
6	6.50	5.03	0.10	1.20	0.71	0.22	29.16	0.64	1.56	1.46
7	5.33	0.66	6.35	7.88	1.09	8.09	31.85	0.71	1.40	1.27
8	4.91	0.95	3.43	4.79	0.47	4.14	31.20	0.72	1.38	1.32
9	**8.88**	**5.40**	**0.21**	**0.88**	**0.50**	**0.27**	**29.83**	**0.61**	**1.63**	**1.44**
10	9.45	4.31	0.10	0.84	0.83	0.45	29.72	0.61	1.63	1.42
11	**7.24**	**4.33**	**0.10**	**1.58**	**1.47**	**0.33**	**28.67**	**0.64**	**1.56**	**1.40**
12	4.21	1.71	2.19	2.86	0.53	1.09	31.15	0.72	1.38	1.46
13	5.95	2.12	1.10	2.08	0.84	1.10	30.32	0.69	1.46	1.33
14	3.67	0.92	1.81	3.21	1.55	3.17	30.98	0.75	1.33	1.47
15	3.72	1.50	1.64	2.81	0.67	1.21	30.47	0.73	1.36	1.53
16	8.82	8.38	0.25	0.44	0.20	0.11	31.08	0.59	1.70	1.54
17	8.30	4.98	0.36	1.21	0.58	0.30	29.66	0.62	1.61	1.42
18	3.71	1.43	0.40	1.59	1.70	1.32	30.11	0.74	1.36	1.52
19	4.47	1.76	0.10	1.31	1.81	1.12	29.76	0.72	1.39	1.43
20	8.43	1.73	4.06	4.78	0.09	2.36	31.55	0.65	1.55	1.32

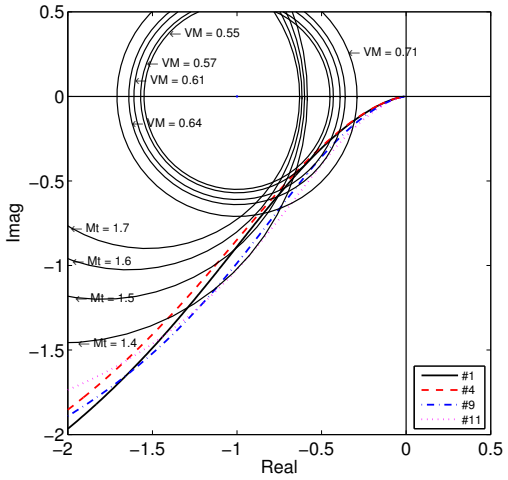

Fig. 17. G_{p1} results. Nyquist plots for the 4 selected solutions.

The results obtained for the PID case, for plant G_{p2}, considering the final set of 20 plants are illustrated in Figs. 18 and 19. Fig. 18 presents the SPT response when an unit step is applied at $t = 0s$, and a DR when a unit step is applied to the load disturbance at $t = 35s$ as well as the respective controller signal output. These figures illustrate that the control engineer may select the solution with best compromise regarding both responses performance. Fig. 19 presents the Nyquist plots obtained for the corresponding 20 loop transfer functions. As it can be observed from these figures, due to the third order pole model in

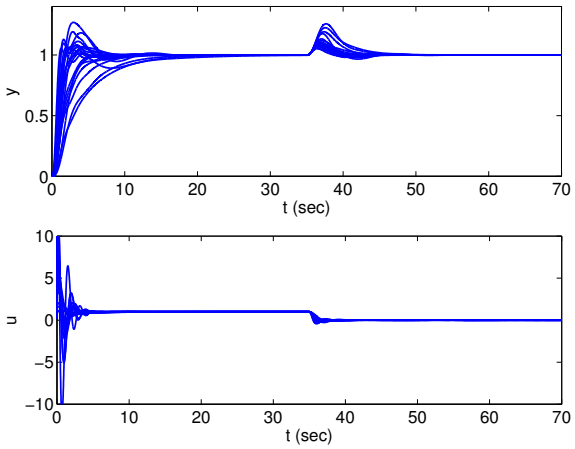

Fig. 18. G_{p2} results. SPT and DR response and Controller output signals for the set of 20 selected solutions.

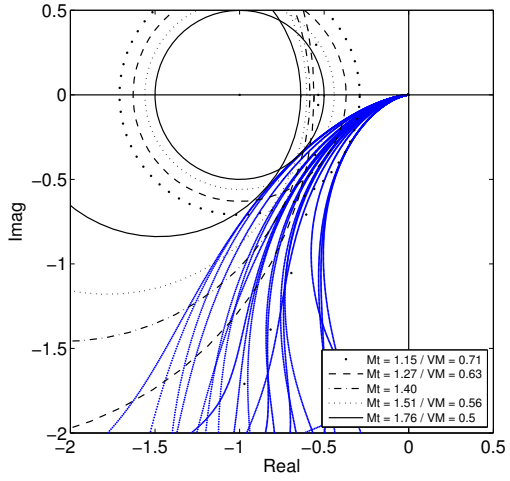

Fig. 19. G_{p2} results. Nyquist plots for the 20 solutions.

question, the Nyquist plots can be rather irregular in terms of its curvature. Table 5 presents the set of values obtained for the PID controller and lead-lag pre-filter, the values obtained regarding the four design objectives considered, and values for M_s and M_t. Table 5 results clearly show that for the case of T_{lead} the variation is minimum, as most cases converged to the minimum interval value of $0.1s$.

6. PID RESULTS COMPARISON

The techniques considered to compare the results achieved with the MaPSO for PID control applied to the system Gp2 are the following:

1) The Cohen-Coon (CC) PID tuning rules [40], presented in (29), where K, T, and L, represent respectively the dc gain, the dominant time constant and the timed delay of a first order plus timed delay (FOPTD) model approximation to the system to be controlled;
2) The Murrill [41] tuning rules based on the ITAE minimization for load disturbance rejection, presented in (30);
3) The Magnitude Optimum for Disturbance Rejection (DRMO) [42].
4) The results presented in [7] based on a technique minimizing the IAE, resulting for system (28) in the following controller settings, when a constraint of $Ms = 1.4$ was used: $Kp = 3.81$, $Ki = 3.33$ and $Kd = 4.25$.

Table 5. Non-dominated front obtained by G_{p2}.

#	variables					objectives				M_s	M_t
	K_p	K_i	K_d	T_{lead}	T_{lag}	ITAE SPT	ITAE LDR	CE	VM		
1	11.76	11.35	10.98	0.10	0.57	1.13	0.33	43.78	0.50	2.00	1.74
2	5.71	4.58	8.28	0.10	1.84	3.30	1.39	36.79	0.63	1.59	1.22
3	11.41	10.36	14.69	0.10	0.24	2.77	0.50	49.67	0.50	1.98	1.71
4	11.23	4.67	8.87	0.15	2.63	6.88	0.58	36.38	0.50	2.00	1.74
5	**8.30**	**2.44**	**6.81**	**0.10**	**0.69**	**0.84**	**1.56**	**39.98**	**0.56**	**1.78**	**1.48**
6	3.37	1.00	2.42	0.10	0.37	1.33	4.37	37.82	0.71	1.40	1.01
7	**3.74**	**1.54**	**3.24**	**1.57**	**2.13**	**2.67**	**2.20**	**37.68**	**0.71**	**1.40**	**1.01**
8	4.32	3.98	7.09	0.10	0.33	5.32	2.19	40.11	0.67	1.48	1.14
9	6.73	6.05	9.03	0.10	2.21	4.65	1.02	36.47	0.60	1.66	1.31
10	2.89	1.00	1.79	0.10	1.40	3.87	3.89	36.89	0.71	1.41	1.03
11	6.67	5.90	8.40	0.10	0.55	2.30	0.98	40.40	0.61	1.64	1.30
12	7.59	5.21	7.97	0.10	4.28	18.35	0.74	34.37	0.59	1.70	1.38
13	7.77	7.73	8.86	0.10	1.11	1.52	0.71	38.31	0.58	1.72	1.39
14	10.37	6.84	10.0	0.10	0.50	1.19	0.48	43.60	0.53	1.90	1.61
15	8.32	3.21	6.63	0.84	1.39	1.64	0.91	38.81	0.56	1.79	1.50
16	5.39	3.22	5.07	1.33	1.42	4.28	1.11	38.46	0.65	1.54	1.19
17	4.84	2.26	2.85	0.10	3.66	14.42	1.15	35.17	0.60	1.69	1.41
18	7.58	4.40	8.53	5.31	7.40	14.37	0.88	36.57	0.59	1.70	1.38
19	5.91	4.24	7.16	0.10	0.96	1.87	1.16	37.97	0.63	1.58	1.22
20	**6.06**	**4.19**	**7.64**	**0.10**	**1.65**	**2.58**	**1.19**	**36.94**	**0.63**	**1.60**	**1.24**

$$
\begin{aligned}
K_p &= \frac{1}{K}\frac{T}{L}\left(\frac{4}{3}+\frac{L}{4T}\right),\\
T_i &= L\frac{32+6\frac{L}{T}}{13+8\frac{L}{T}},\\
T_d &= L\frac{4}{11+2\frac{L}{T}},
\end{aligned}
\tag{29}
$$

$$
\begin{aligned}
K_p &= \frac{1.357}{K}\left(\frac{L}{T}\right)^{-0.947},\\
T_i &= \frac{T}{0.842\left(\frac{L}{T}\right)^{-0.738}},\\
T_d &= 0.381T\left(\frac{L}{T}\right)^{0.995}.
\end{aligned}
\tag{30}
$$

As the proposed MaPSO considers equally relevant the optimization of 4 different criteria: ITAE minimization for SPT, ITAE minimization for load DR, CE minimization, VM maximization, the procedure adopted for comparing with the Cohen and Coon and Murril ITAE methods is the following:

- Obtain the FOPTD model approximation using the two-point open-loop identification method [43]. For the third-order pole system this approximation results in the following settings: $K = 1$; $T = 1.74s$; $L = 1.47s$;
- Evaluate the Cohen-Coon controller settings using (29) which converted to the ideal controller format used in this study (30) results in the following settings: $Kp_{cc} = 1.19$, $Ki_{cc} = 0.64$ and $Kd_{cc} = 0.55$. Determine the corresponding robustness values achieved with this controller gain set: $VM = 0.73$, $Ms = 1.34$, $Mt = 1.06$.
- Evaluate the ITAE controller settings using (30), which converted to the ideal controller format used in this study (30) results in the following settings: $Kp_{itae} = 1.56$, $Ki_{itae} = 0.88$ and $Kd_{itae} = 0.89$. Determine the corresponding robustness values achieved with this controller gain set: $VM = 0.71$, $Ms = 1.4$, $Mt = 1.01$.
- From the 20 non-dominated solutions obtained with the proposed MaPSO, presented in Table 5, select one with has the most similar value in terms of vector margin (VM) and compare the results terms of LDR responses and well as CE values. As the design proposed with MaPSO used a lead-lag input reference pre-filter, the values obtained with the MaPSO are used for the CC and ITAE rules simulation.
- As the maximum value obtained for VM with the MaPSO was 0.71, with 3 of the 20 non-dominated solutions (see Table 5) presenting the same value (#6, #7, #10) and similar Mt values, solution #7 is selected as it present better balancing between the SPT and LDR values.

The comparison results between MaPSO, Cohen and Coon tuning and Murril ITAE rules are presented in Figure 20 and Table 6. As it can be observed the results show that the MaPSO solution performs much better for LDR than the Cohen-Coon and ITAE tuning rules in terms of the ITAE, requiring a slightly higher control effort.

Regarding the comparison with the DRMO [42] method, the obtained PID gains are: $Kp = 2.95$; $Ki = 1.74$ and $Kd = 1.5$, resulting in values for $VM = 0.58$ ($M_s = 1.72$) and $M_t = 1.48$. The closest solution obtained with the MaPSO is solution #5 with VM=0.56 and Mt=1.48. The results comparing these two methods are presented in Fig. 21, and Table 6. As it can be observed the MaPSO solution outperforms the DRMO method for LDR requiring similar control effort.

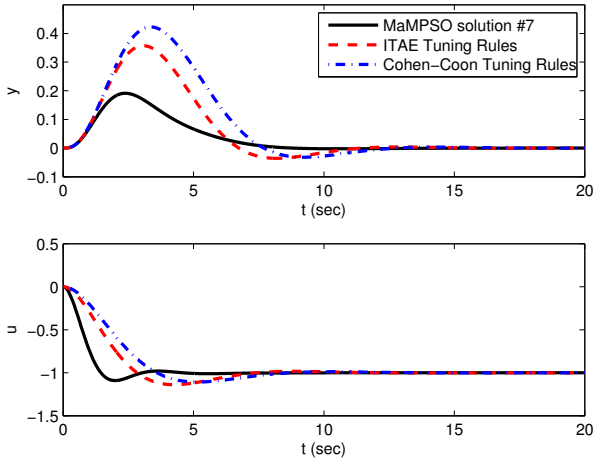

Fig. 20. MaPSO versus Cohen-Cohen and Murrill rules for Gp2. Load disturbance rejection (LDR) responses when a unit step is applied $d = 1$ is applied at $t = 0$s.

Table 6. Comparison between MaPSO solution #7, Cohen-Coon and Murril ITAE for Gp2.

Method	Kp	Ki	Kd	ITAE LDR	ITAE STP	CE LDR	VM	M_s	M_t
MaMPSO (#7)	3.74	1.54	3.24	2.20	2.68	19.36	0.71	1.4	1.01
Cohen-Coon	1.19	0.64	0.55	7.11	5.34	18.45	0.73	1.38	1.01
ITAE (Murril)	1.56	0.88	0.89	5.07	4.94	18.86	0.73	1.38	1.12
MaMPSO (#5)	8.30	2.44	6.81	2.20	2.68	19.60	0.56	1.78	1.01
DRMO	2.95	1.74	1.5	2.45	4.17	19.43	0.58	1.72	1.48
MaMPSO (#20)	6.06	4.19	7.64	1.12	2.56	19.77	0.63	1.59	1.23
Hast et al. [7]	3.81	3.33	4.25	2.00	6.33	19.70	0.72	1.4	1.26

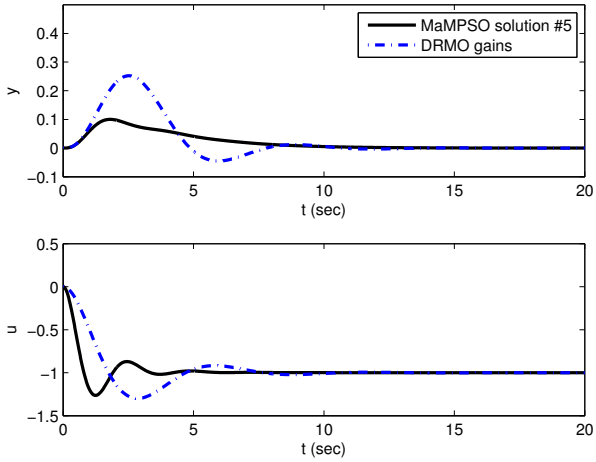

Fig. 21. MaPSO versus DRMO method for Gp2. Load disturbance rejection (LDR) responses when a unit step is applied $d = 1$ is applied at $t = 0s$.

Concerning the comparison with the ITAE optimization method proposed by Hast et al. [7], it is important to men-

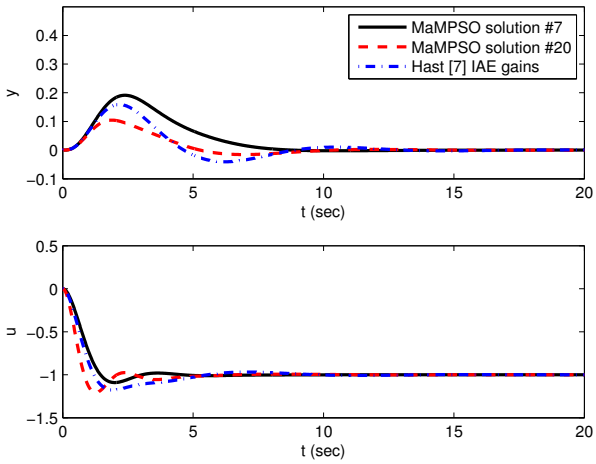

Fig. 22. MaPSO versus IAE minimization for LDR by Hast et al. [7] for Gp2. Load disturbance rejection (LDR) responses when a unit step is applied $d = 1$ is applied at $t = 0s$.

tion that while the controller gains achieved in [7] consider solely a maximum sensitivity constraint. The comparison results presented in Figure 22 and Table 6, consider two MaPSO solution #7 and #20. While solution#7 present very similar values in terms of the VM it performs worst in terms of the ITAE for LDR. However, as it can be observed from Table 6, the maximum sensitivity values are quite different. Considering solution #20 which presents a similar Mt value to the one presented by the Hast solution, with a smaller VM, the performance in terms of ITAE for LDR is better for the MaPSO approach.

7. CONCLUSION

In this paper two particle swarm optimization algorithm based techniques were proposed to address the problem of designing PI-PID controllers fulfilling minimum robustness properties. The two reported techniques are: i) a single-objective PSO optimization technique, to sequentially design PI-PID controllers firstly to deal with load disturbance rejection. Then design a lead-lag pre-filter in a two degrees-of-freedom configuration with the fixed feedback loop, in order to optimize the system load disturbance rejection; The robustness constraints used are based on vector margin and maximum complementary sensitivity circles constraints. ii) A many-objective optimization technique that optimizes simultaneously four different design criteria. The design criteria considered are: set-point tracking, load disturbance rejection, control effort minimization, maximization of the vector margin. Simulation results were presented for both single and many objective optimization approaches, which show the benefits of the proposed PI-PID design techniques, in comparison with both classic and optimization methods.

REFERENCES

[1] A. O'Dwyer, *Handbook of PI and PID Controller Tuning Rules*, 2nd Edition, Imperial College Press, 2006.

[2] D. Vrančić, S. Strmčnik and Đ. Juričić, "A magnitude optimum multiple integration tuning method for filtered PID controller," *Automatica*, vol. 37, no. 9, pp. 1473-1479, 2001. [click]

[3] K. J. Åström and T. Hägglund, "The future of PID control," *Control Engineering Practice*, vol.9, no. 11, pp. 1163-1175, 2001.

[4] S. Skogestad, "Simple analytic rules for model reduction and PID controller tuning," *Modeling, Identification and Control*, vol. 25, no. 2, pp. 85–120, 2004. [click]

[5] M. G. Lin, S. Lakshminarayanan, and G. P. Rangaiah, "A Comparative Study of Recent/Popular PID Tuning Rules for Stable, First-Order Plus Dead Time, Single-Input Single-Output Processes," *Industrial & Engineering Chemistry Research*, vol. 47, no. 2, pp. 344-368, 2008. [click]

[6] W. Cho, J. Lee, and T. F. Edgar, "Simple Analytic Proportional-Integral-Derivative (PID) Controller Tuning Rules for Unstable Processes," *Industrial & Engineering Chemistry Research*, vol. 53, no. 13, pp. 5048-5054, 2014. [click]

[7] M. Hast, K.J. Åström, B. Bernhardsson, S. Boyd, "PID design by convex-concave optimization," *Proc. of Control Conference (ECC), 2013 European*, IEEE, pp. 4460-4465, July 2013.

[8] C. M. Fonseca and P.J. Fleming, "Multiobjective optimal controller design with genetic algorithms," *Proc. of Control, 1994. Control '94. International Conference on*, vol. 1, pp. 745-749, March 1994.

[9] A. H. Jones and P. B.de Moura Oliveira, "Genetic auto-tuning of PID controllers," *Proc. of Genetic Algorithms in Engineering Systems: Innovations and Applications, 1995. GALESIA. First International Conference on (Conf. Publ. No. 414)*, pp. 141-145, Sheffield, September 1995.

[10] A. Herreros, E. Baeyens, and J. R. Perán, "Design of PID-type controllers using multiobjective genetic algorithms," *ISA Transactions*, vol. 41, no. 4, pp. 457-472, 2002. [click]

[11] P.B. de Moura Oliveira, "Modern heuristics review for PID control optimization: a teaching experiment," *Proc. of Control and Automation, 2005. ICCA '05. International Conference on*, vol. 2, pp. 828-833, June 2005.

[12] P. B. de Moura Oliveira, J. B. Cunha, and J. P. Coelho, "Design of PID controllers using the particle swarm algorithm," *Proc. of IASTED MIC'2002*, pp. 263-268, Innsbruck, Austria, February 2002.

[13] J.-Y. Cao and B.-G. Cao, "Design of fractional order controllers based on particle swarm optimization," *International Journal of Control, Automation, and Systems*, vol. 4, no. 6, pp.775-781, 2006.

[14] P. B. de Moura Oliveira, E. J. Solteiro Pires, J. B. Cunha, and D. Vrančić, "Multi-Objective Particle Swarm Optimization Design of PID Controllers", *Distributed Computing, Artificial Intelligence, Bioinformatics, Soft Computing, and Ambient Assisted Living*, Springer Berlin Heidelberg, vol. 5518 of the series Lecture Notes in Computer Science, editor S. Omatu and *et. al.*, pp. 1222-1230, 2009.

[15] S.-Z. Zhao,M. W. Iruthayarajan, S. Baskar, and P.N. Suganthan, "Multi-objective robust {PID} controller tuning using two lbests multi-objective particle swarm optimization," *Information Sciences*, vol. 181, no. 16, pp. 3323-3335, 2011. [click]

[16] R. Dong, "Differential evolution versus particle swarm optimization for PID controller design," *Proc. of Natural Computation, 2009. ICNC '09. Fifth International Conference on*, vol. 3, pp. 236-240, August 2009.

[17] P. B. de Moura Oliveira, E. J. Solteiro Pires, and P. Novais, "Gravitational Search Algorithm Design of Posicast PID Control Systems," *Soft Computing Models in Industrial and Environmental Applications*, Springer International Publishing, vol. 188 of the series Advances in Intelligent Systems and Computing, editor V. Snášel *et.al.*, pp. 191-199, 2013.

[18] P. B. de Moura Oliveira, H. Freire, E.J. Solteiro Pires, and J. B. Cunha, "Bridging Classical Control with Nature Inspired Computation Through PID Robust Design," *Proc. of 10th International Conference on Soft Computing Models in Industrial and Environmental Applications*, Springer International Publishing, vol. 368 of the series Advances in Intelligent Systems and Computing, editor A. Herreno *et. al.*, pp. 307-316, 2015.

[19] H. Freire, P. B. de Moura Oliveira, E. J. Solteiro Pires, and M. Bessa, "Many-Objective PSO PID Controller Tuning," *Controlo'2014 - Proceedings of the 11th Portuguese Conference on Automatic Control*, Springer International Publishing, vol. 321 of the series Lecture Notes in Electrical Engineering, editor A. P. Moureira *et. al.*, pp. 183-192, 2015.

[20] I. Chiha, N. Liouane, and P. Borne, "Tuning PID Controller Using Multiobjective Ant Colony Optimization," *Proc. of Appl. Comp. Intell. Soft Computing*, vol. 2012, 2012.

[21] V. Rajinikanth and K. Latha, "Tuning and retuning of PID controller unstable systems using evolutionary algorithm," *Appl. Comp. Intell. Soft Comput.*, vol. 2012, 2012.

[22] H. Freire, P. B. de Moura Oliveira, E. J. Solteiro Pires, and M. Bessa, "Many-objective optimization with corner-based search," *Memetic Computing*, Springer Berlin Heidelberg, vol. 7, no. 2, pp. 105-118, 2015.

[23] K. Deb, S. Agrawal, A. Pratap, and T. Meyarivan, "A fast and elitist multiobjective genetic algorithm: NSGA-II," *IEEE Trans. Evolutionary Computation*, vol. 6, no. 2, pp. 182-197, 2002.

[24] A. J. Nebro, j. J. Durillo, J. Garcia-Nieto, C. A. Coello Coello, F. Luna, and E. Alba, "SMPSO: A new PSO-based metaheuristic for multi-objective optimization," *Proc. of Computational intelligence in miulti-criteria decision-making, 2009. MCDM '09. IEEE symposium on*, pp. 66-73, 2009.

[25] S. Kukkonen and J. Lampinen, "GDE3: the third evolution step of generalized differential evolution," *Evolutionary Computation, 2005. The 2005 IEEE Congress on*, vol. 1, pp. 443-450, 2005.

[26] V. R. Segovia, Vanessa, T. Hägglund, and K. J. Åström, "Noise filtering in PI and PID Control", *2013 American Control Conference*, IEEE, pp. 1763-1770, 2013.

[27] Hägglund, T., "Signal Filtering in PID Control," *IFAC Conf. Advances in PID Control*, vol. 12, 2012.

[28] M. Araki and H. Taguchi, H., "Two-Degree-of-Freedom PID Controllers," *International Journal of Control, Automation, and Systems*, vol. 1, no. 4, pp. 401-411, 2003.

[29] K. J. Åström and T. Hägglund, "PID Control," *The Control Handbook*, Edit. Levine W. S., CRC-IEE Press, pp. 198-208, 1996.

[30] O. Smith, *Feedback Control Systems*, McGraw-Hill, pp. 198-208, 1958.

[31] G. F. Franklin, D. J. Powell, and A. Emami-Naeini, *Feedback Control of Dynamic Systems*, Prentice Hall PTR, 4th edition, 2001.

[32] J. Kennedy and R. Eberhart, "Particle swarm optimization," *Neural Networks, 1995. Proceedings., IEEE International Conference on*, IEEE, Australia, vol. 4, pp. 1942-1948, 1995.

[33] X. Chen and Y. M. Li, "On convergence and parameter selection of an improved particle swarm optimization," *International Journal of Control Automation and Systems*, vol. 6, no. 4, pp. 559-570, 2008.

[34] G. Shahgholian, A. Movahedi, and J. Faiz, "Coordinated design of TCSC and PSS controllers using VURPSO and Genetic algorithms for multi-machine power system stability," *International Journal of Control, Automation and Systems*, vol. 13, no. 2, pp. 398-409, 2014. [click]

[35] J. C. Bansal, P. K. Singh, M. Saraswat, A. Verma, S. S. Jadon, and A. Abraham, "Inertia weight strategies in particle swarm optimization," *Proc. of Nature and Biologically Inspired Computing (NaBIC), 2011 Third World Congress on*, pp. 633-640, 2011.

[36] C. A. Coello Coello, G. L. Lamont, and D. A. van Veldhuizen, *Evolutionary Algorithms for Solving Multi-Objective Problems*, 2nd edition, Springer, series of the Genetic and Evolutionary Computation, 2007.

[37] E. J. Solteiro Pires, P. B. de Moura Oliveira, and J. A. Tenreiro Machado, "Multi-objective MaxiMin Sorting Scheme", *Evolutionary Multi-Criterion Optimization*, series of the Lecture Notes in Computer Science, Springer Berlin Heidelberg, editors C. A. Coello Coello *et. al.*, vol. 3410, pp. 165-175, 2005.

[38] K. Deb, *Multi-Objective Optimization using Evolutionary Algorithms*, John Wiley & Sons, UK, 2001.

[39] C. C. Coello, G. B. Lamont, and D. A. Van Veldhuizen, *Evolutionary Algorithms for Solving Multi-Objective Problems (Genetic and Evolutionary Computation)*, Springer-Verlag New York, Inc., USA, 2006.

[40] G. Cohen and G. Coon, "Theoretical consideration of retarded control," *Trans. of American society of Mechanical Engineers, ASME 75*, pp. 827-834, 1953.

[41] P. W. Murrill, "Automatic Control of Processes," *International Textbooks in Chemical Engineering*, International Textbook Company, 1967.

[42] D. Vrančić, S. Strmčnik, J. Kocijan, and P.B. de Moura Oliveira, "Improving disturbance rejection of PID controllers by means of the magnitude optimum method," *ISA Transactions*, vol. 49, no. 1, pp. 47-56, 2010.

[43] K. R. Sundaresan and P. R. Krishnaswamy, "Estimation of time delay time constant parameters in time, frequency, and laplace domains," *The Canadian Journal of Chemical Engineering*, Wiley Subscription Services, Inc., A Wiley Company, vol. 56, no. 2, pp. 257-262, 1978.

Hélio Freire received the Licence degree in 2009 and the MSc in evolutionary algorithms in 2011, both from the University of Trás-os-Montes e Alto Douro (UTAD), Portugal. He is a researcher at the INESC TEC institute and a PhD student with the UTAD. His research interests include evolutionary computation for multi-objective problems and PID control.

P. B. Moura Oliveira received the Electrical Engineering degree in 1991, from the UTAD University, Portugal, MSc in Industrial Control Systems in 1994 and PhD in Control Engineering in 1998, both from Salford University, Manchester, UK. He is an Associated Professor with Habilitation at the Engineering Department of UTAD University and a researcher at the INESC TEC institute. Currently, he is the director of the PhD Course in Electrical and Computers Engineering in UTAD. His research interests are focused on the fields of control engineering, intelligent control, PID control, control education, evolutionary and natural inspired algorithms for single and multiple objective optimization problem solving. He is author in more than 100 peer-reviewed scientific publications.

E. J. Solteiro Pires received the degree in Electrical Engineering at the University of Coimbra, in 1993. He pursued post graduate studies and obtained, in 1999, an MSc degree in Electrical and Computer Engineering at the University of Oporto. In 2006, he graduated with a PhD degree at UTAD University. Since 2006 he works as an Assistant Professor at the Engineering Department of UTAD University. His main research interests are in evolutionary computation, multi-objective problems, fractional calculus, and diffusion of innovation.